25 Gb/s Direct Modulation of Implant-Confined Holey VCSELs

Chen Chen[1*], Zhaobing Tian[1], Kent D. Choquette[2] and David V. Plant[1]
[1]Dept. of Electrical and Computer Engineering, McGill University, Montreal, QC, Canada
[2]University of Illinois, Urbana, IL, USA
*chen.chen4@mail.mcgill.ca

Abstract: 25 Gb/s direct modulation and bit error measurements over 100m multimode fiber from an 850-nm implant-confined holey VCSEL are demonstrated. The high speed performance arises from cavity designs that are achieved using standard fabrication and epitaxial materials.

OCIS codes: (140.9560) Semiconductor Lasers (140.7260) Vertical Cavity Surface Emitting Lasers

I. Introduction

The modulation characteristics of implant-confined photonic crystal (PhC) and/or holey vertical-cavity surface-emitting lasers (VCSELs) have been studied in the prior work [1-2]. Despite a maximum small-signal bandwidth of 18 GHz, the large-signal performance of holey VCSELs can be hindered by the carrier diffusion effect arising from the size difference between the electrical and optical apertures, which makes it difficult to relate the laser small- and large-signal characteristics [2]. A small aperture size difference (less than 4 μm in diameter) enables to minimize the carrier diffusion effect and to achieve large-signal modulation at higher data rates [2]. In this work, 25 Gb/s operation of an implant-confined holey VCSEL is achieved with a low operation current density of 7.4 KA/cm^2. The device design parameters, small-signal characteristics and bit-error-ratio (BER) results are presented.

The VCSEL is a suitable laser source for short-haul communication networks, due to its ability for low-cost high-volume manufacture, low power consumption and other unique advantages [3]. High-speed direct modulation of a VCSEL is desired to further increase the transmission capacity of communication networks. Various approaches have been employed to improve the direct modulation bandwidth of a VCSEL [1, 4-7], and the highest data rate reported is 35 Gb/s using a 980-nm tapered-oxide VCSEL [4]. The incorporation of a holey structure into a VCSEL enables to engineer the transverse lasing modes and effectively reduce the optical modal volume, while it still maintains a relatively large electrical aperture to ensure a low operation current density. This makes it a promising approach for VCSELs to achieve high speed modulation and high reliability simultaneously. Moreover, our approach is independent of the epitaxial design, and thus can be combined with other methodologies to increase modulation bandwidth even further.

II. Device structure and dc properties

Fig. 1(a) illustrates the cross-section schematic of a PhC VCSEL. The proton implant-confined VCSELs were fabricated from a wafer with conventional 850-nm epitaxy design. Coplanar ground-signal-ground contacts were deposited on planarized polyimide to reduce parasitic capacitance and facilitate on-wafer high-speed measurement [1]. The PhC structures were defined using electron beam lithography and etched approximately 16 periods (out of 21 total periods) into the top distributed Bragg reflector [1]. Fig. 1(b) shows the optical image of the VCSEL supporting 25 Gb/s operation reported in this work. This particular VCSEL has a 11-μm diameter implant aperture, and the PhC lattice constant a = 6 μm and hole diameter b = 3.6 μm (or b/a = 0.6), resulting in an optical aperture diameter of 8.4 μm. The aperture size difference is 2.6 μm in diameter, and thus the carrier diffusion effect is expected to diminish. Note that the VCSEL contains only a single period of the PhC pattern and this lack of periodicity makes it a holey VCSEL to be exact.

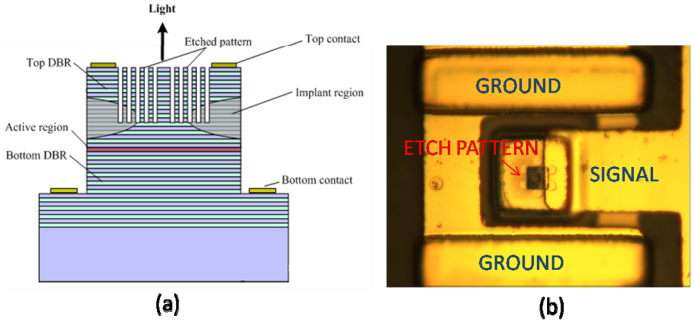

Fig. 1: (a) Cross-section schematic and (b) optical image of the PhC VCSEL.

978-1-55752-884-1/10/$26.00 ©2010 IEEE

Fig. 2(a) shows the continuous-wave light-current-voltage (LIV) characteristics of the holey VCSEL at room-temperature. The VCSEL has a threshold current of 1.8 mA, and a series resistance of 57.6 Ω between 7 and 12 mA. Figure 2(b) illustrates the optical spectrum of the VCESL taken at dc current of 9 mA with and without the 25 Gb/s modulation. Three transverse optical modes are observed. With the 25 Gb/s modulation, the optical spectrum shifts to a longer wavelength by 0.3 nm and broadens, and the maximum power in the spectrum decreases by approximately 3 dB.

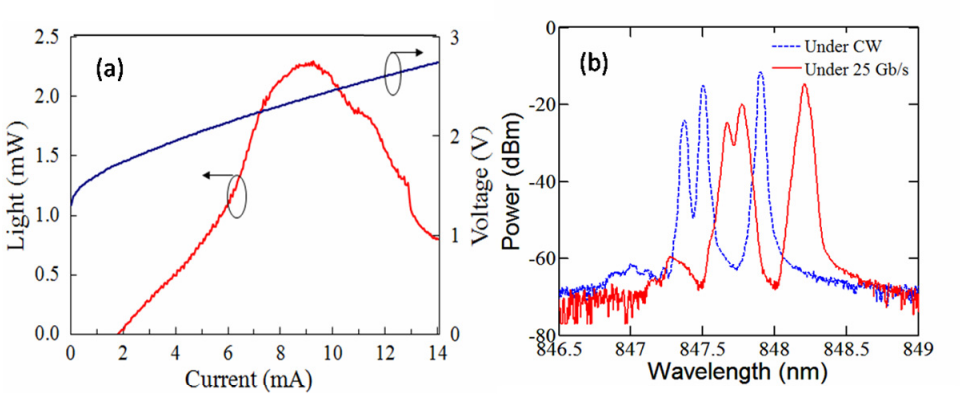

Fig. 2: (a) LIV and (b) optical spectrum of the PhC VCSEL.

II. Small- and large-signal characteristics

For high-speed modulation characterization, a lensed 50/125-μm graded-index (GI) multimode fiber (MMF) and a 25 GHz photodetector are used to collect output light from the holey VCSEL under test. For the small-signal modulation, the modulation voltage is supplied from a network analyzer via a 40 GHz ground-signal-ground microwave probe. For the large-signal modulation, the modulation voltage is supplied from a pattern generator producing a nonreturn to zero pseudorandom bit sequence of 2^7-1. For a back-to-back measurement, a 4-m 50/125-μm GI MMF is used; then a 100-m 50/125-μm GI MMF (i.e. OM2 fiber) is added to evaluate link performance over a longer distance. The eye diagrams are measured with an 80 GHz sampling oscilloscope. BER measurement is taken with an error detector, and two stages of broadband electrical amplifiers are used following the 25 GHz photodetector.

Fig. 3(a) shows the small-signal modulation characteristics of the holey VCSEL at different dc currents. The maximum modulation bandwidth of 15.5 GHz is achieved at 10 mA. Fig. 3(b) illustrates the relaxation oscillation (RO) frequency versus the square root of the dc current above the threshold current. The modulation current efficiency factor (MCEF) is 5.03 GHz/mA$^{1/2}$, and the RO frequency starts to saturate at the dc current of 7 mA. The electrical and optical aperture size difference needs to be accounted, in order to directly compare the MCEF of the holey VCSEL to that of the conventional VCSEL structure. In this case, the effective MCEF is 6.59 GHz/mA$^{1/2}$, similar to those reported for GaAs VCSELs in prior work [7].

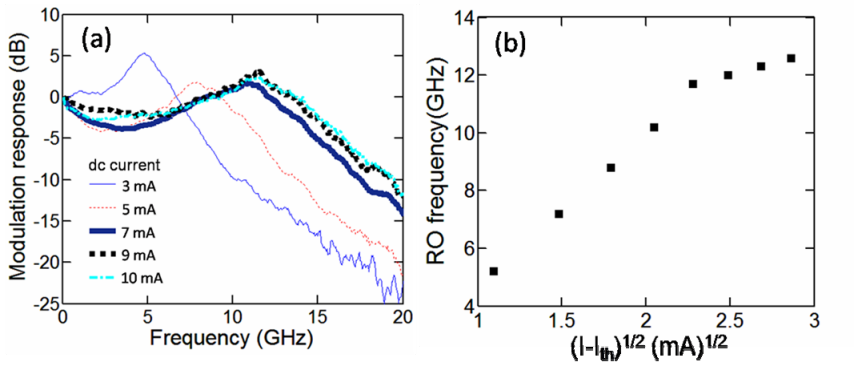

Fig. 3: (a) Small-signal modulation characteristics and (b) RO frequencies with varying dc currents.

Fig. 4 illustrates the eye diagrams of the holey VCSEL under 25 Gb/s operation after a back-to-back and 104-m MMF transmission, respectively. The holey VCSEL is biased at 9 mA, and the peak-peak modulation voltage is 1 V. For the back-to-back (104-m MMF) transmission, the rise and fall time are 19.6 ps and 21.8 ps (29.3 ps and 28.9 ps),

and the extinction ratio is 3.9 dB (3.08 dB). The deteriorated rise/fall time and the extinction ratio after the 104-m transmission are primarily due to the modal dispersion in the MMF. Fig. 5 illustrates the BER versus the received optical power for the both transmission conditions. The lowest BER for back-to-back and 104-m transmission length is 6.8×10^{-11} and 2.47×10^{-8}, respectively, and a power penalty of 0.8 dB is observed. It is important to note that, the current density of the holey VCSEL at 25 Gb/s is only 7.4 KA/cm^2 owing to its large implant aperture size. This operation current density is considerably lower than that from other high speed VCSEL technologies [4-7], and thus substantial improvement of VCSEL reliability should be expected [8].

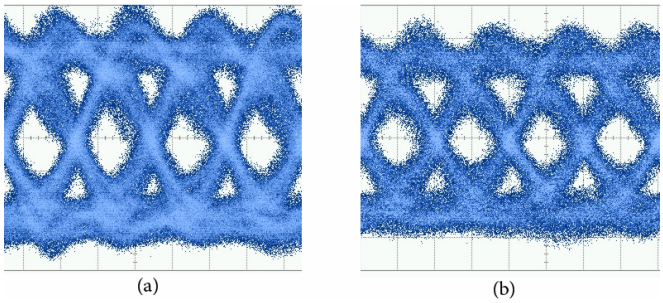

(a) (b)

Fig. 4: Eye diagram of the holey VCSEL under 25 Gb/s modulation after (a) back-to-back (b) 104-m MMF transmission (Horizontal 20 ps/div, Vertical 85.6 mV/div).

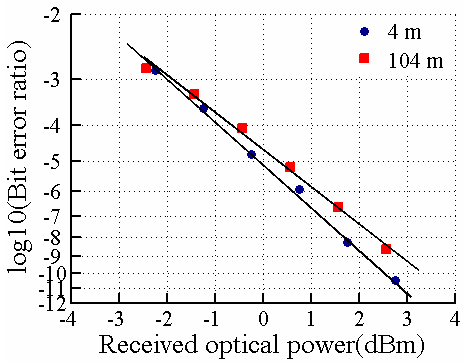

Fig. 5: BER versus received optical power after a transmission over a 4-m and 104-m MMF.

IV. Conclusion

In this work, we demonstrate 25 Gb/s direct modulation of an implant-confined holey VCSEL with a low operation current density of 7.4 KA/cm^2. The small-signal modulation characteristics and the BER measurement for a 100-m MMF link are also presented. With an appropriate PhC and/or holey design, the size of the optical cavity can be reduced independent from that of the electrical cavity, enabling to achieve high speed operation and high laser reliability at the same time. Moreover, the PhC approach can be combined with other optimization methodologies or implemented at other wavelengths for high speed modulation operation.

References:

[1] P. O. Leisher, C. Chen, J. D. Sulkin, M. S. B. Alias, K. A. M. Sharif and K. D. Choquette, "High modulation bandwidth implant-confined photonic crystal vertical cavity surface emitting laser," *IEEE Photon. Technol. Lett.*, vol. 19, no. 19, pp. 1541–1543, 2007.

[2] C. Chen, P. O. Leisher, D. M. Kuchta and K. D. Choquette, "High-speed modulation of index-guided implant-confined vertical cavity surface emitting lasers," *IEEE J. Sel. Topics Quantum Electron.*, vol. 15, no. 3, pp. 673–678, 2009.

[3] K. D. Choquette and K. M. Geib, "Fabrication and performance of vertical-cavity surface-emitting lasers," in *Vertical-Cavity Surface-Emitting Lasers*, C. Wilmsen, H. Temkin, and L. Coldren, Eds. New York: Cambridge Univ. Press, 1999. pp.193-232.

[4] Y. C. Chang, C. S. Wang, L. A. Coldren, *Electron. Lett.*, vol. 43, no. 19, 2007.

[5] T. Anan, N. Suzuki, K. Yashiki, K. Fukatsu, H. Hatakeyama, T. Akagawa and M. Tsuji, Fiber Communication Conference, San Diego, CA, Mar. 2008.

[6] R. H. Johnson and D. M. Kutcha, Conference of Lasers and Electro Optics, San Jose, CA, 2008.

[7] P. Westbergh, J. S. Gustavsson, A. Haglund, H. Sunnerud, and A. Larsson, "High-speed, low-current-density 850 nm VCSELs," *IEEE J. Sel. Topics Quantum Electron.*, vol. 15, no. 3, pp. 694–703, 2009.

[8] B. M. Hawkins, R. A. Hawthorne, J. K. Guenter, J. A. Tatum and J. R. Biard, "Reliability of various size oxide aperture VCSELs," Electronic Components and Technology Conference, San Diedo, CA, 2002.